Light-Gated Control of Conformational Changes in Polymer Brushes

Sabrina Bialas, Tim Krappitz, Sarah L. Walden, Kubra Kalayci, Daniel Kodura, Hendrik Frisch, Jennifer M. MacLeod, Andrew Nelson, Lukas Michalek,* and Christopher Barner-Kowollik**

Herein, a strategy to control conformational changes in grafted polymer brushes via photoinduced crosslinking of photoreactive groups embedded into the lateral architecture of a polymer brush is reported. Poly(methylmethacrylate)-based polymer brushes containing UV-light (λ = 325 nm) photoreactive *o*-methyl benzaldehyde moieties are synthesized using surface-initiated reversible deactivation polymerization. The conformational changes in polymer brushes upon UV-light triggered crosslinking are comprehensively analyzed through a full suite of surface sensitive characterization methods including time of flight secondary ion mass spectrometry, quartz crystal microbalance with dissipation monitoring, UV/vis spectroscopy, atomic force microscopy, nanoplasmonic sensing, and neutron reflectometry. The spatiotemporal control of the induced conformational changes is demonstrated via photolithography experiments. To enable an additional level of control, a second gate, the visible light (λ = 445 nm) active styrylpyrene moiety, is incorporated into the polymer brush architecture. Critically, wavelength-selective crosslinking behavior is observed in the diblock copolymer structures allowing to crosslink specific sections of the lateral brush architecture as a function of irradiation wavelength.

1. Introduction

The vast majority of interactions between materials and their surroundings are governed by their surfaces.[1] Thus, designing and tailoring material surfaces is a critical exercise. Functionalized surfaces span applications from medical technology[2,3] to electronics[4] and coatings.[5–7] One approach to modify the surface properties of substrates, such as their hydrophobicity,[8,9] anti-biofouling[7] or tribology,[10] involves covalently tethering polymer chains onto the surface, commonly known as polymer brushes. The interaction of the functionalized surface with its environment is determined by the chemical composition, as well as the length and density, of the polymeric chains that are tethered to the surface.[11,12] In particular, the mass density of a polymer brush and the distance between the tethering sites, referred to as grafting density, strongly affect the surface properties of the functionalized substrate.[11,12] The chemical composition of a polymer brush can be tailored toward desired material properties by incorporating functional monomers into the polymer chains. The surface functionalization can either be achieved by tethering end-functionalized polymers onto surfaces in a process known as "grafting-to," or polymer brushes can be grown in situ, from a surface-functionalized substrate, which is known as "grafting-from."[11] Since the latter "grafting-from" approach only requires diffusion of monomers to the active site, instead of transporting large polymer chains, it generally enables the formation of denser and thicker polymer brushes compared to the "grafting-to" approach.[11] However, once a polymer brush has been formed on a surface, it is challenging to adjust its conformation and accompanying properties. For the ready applicability of polymer brushes in many technologies (e.g., microelectronics),[13] the spatiotemporal controlled change of surface properties post-manufacturing is desirable.

A few examples of changes to the polymer brush conformation postfunctionalization span from temperature induced collapse of polymer brushes,[14] to pH tuneable conformational changes,[15] and interchain crosslinking.[16] Recently, Mocny and Klok explored the reversible crosslinking of polymer brushes using interchain disulfide bonds.[17] The crosslinking of the polymer brushes was achieved by heating the polymer brushes to 60 °C under air, whereas the decrosslinking was achieved by exposing the initially formed disulfide bridges to

S. Bialas, Dr. T. Krappitz, Dr. S. L. Walden, K. Kalayci, D. Kodura, Dr. H. Frisch, Prof. J. M. MacLeod, Dr. L. Michalek, Prof. C. Barner-Kowollik
School of Chemistry and Physics
Queensland University of Technology (QUT)
2 George Street, Brisbane, QLD 4000, Australia
E-mail: lukas.michalek@qut.edu.au; christopher.barnerkowollik@qut.edu.au
S. Bialas, Dr. T. Krappitz, Dr. S. L. Walden, K. Kalayci, D. Kodura, Dr. H. Frisch, Prof. J. M. MacLeod, Dr. L. Michalek, Prof. C. Barner-Kowollik
Centre for Materials Science
Queensland University of Technology (QUT)
2 George Street, Brisbane, QLD 4000, Australia
Dr. A. Nelson
Australian Nuclear Science and Technology Organisation (ANSTO)
Locked Bag 2001, Kirrawee DC, NSW 2231, Australia
E-mail: andrew.nelson@ansto.gov.au

a chemical trigger, tris(2-carboxyethyl)phosphine hydrochloride, releasing free thiol groups. Other examples of conformation changes in polymer brush structures, and their properties, via crosslinks, are based on the complexation of ions or low molecular guests,[18] the addition of bis(Pd^{II}-pincer) complexes[19] or urea,[20] depending on the functional moieties attached to the polymer. Further examples in the literature demonstrate that interchain crosslinking of polymer brushes can successfully enhance the robustness and improve the mechanical properties of polymer brushes postmanufacturing.[21–23] However, stimuli such as temperature and chemical reagents provide no spatial resolution over the induced changes in brush conformation, which prevents 2D resolved crosslinking of the polymer brushes. The lack of control over polymer brush conformations in surface patterning results in scarce utilization in real world applications. By accomplishing spatiotemporal control over surface properties through conformational changes in grafted polymer chains, improved applicability of polymer brushes in a wide range of technologies can be accomplished. One avenue to achieve comprehensive control over polymer brush conformation is by employing light-gated, interchain crosslinking to modify the brush architecture.

Photochemical reactions provide facile access to spatiotemporal and wavelength-selective reaction control,[24] resulting in a plethora of manufacturing applications such as additive manufacturing and 2D lithography. Polymer brushes find particular utilization in the field of photopatterning due to the ability to selectively incorporate chemical functionalities during the synthetic procedure.[25] Through improved synthetic protocols and advanced manufacturing technologies, patterned surfaces with multiple polymer brushes can be fabricated.[26,27] The applications range from hypersurfaces,[28–30] to microelectronics[13] and antimicrobial surfaces.[31] To extend the photopatterning approach even further, the incorporation of photoreactive moieties to alter the surface properties postmanufacturing would be beneficial.

Recently, our group demonstrated that photochemically induced surface ligation reactions give access to wavelength selective control over grafting densities.[32] In this work, we expand the spatiotemporal control of light-gated reactions into polymer brushes. We herein develop a photochemical crosslinking approach to induce conformation changes in polymer brushes by incorporating photoreactive groups into the lateral brush architecture (**Scheme 1**). The light-gated conformation changes were characterized with a comprehensive suite of characterization methods including UV–vis spectroscopy (UV/vis), atomic force microscopy (AFM), neutron reflectometry (NR), and quartz crystal microbalance with dissipation monitoring (QCM-D). The introduced technology can be readily employed to surface pattern polymer brushes. We report the implementation of photochemical gates (*o*-methyl benzaldehyde (*o*-MBA) and styrylpyrene (StyP) moieties) into either monoblock (**MB**) or diblock (**DB**) copolymer brushes. In doing so, we present an additional dimension of control over the internal structure of polymer brush conformation via photocrosslinking reactions, postmanufacturing.

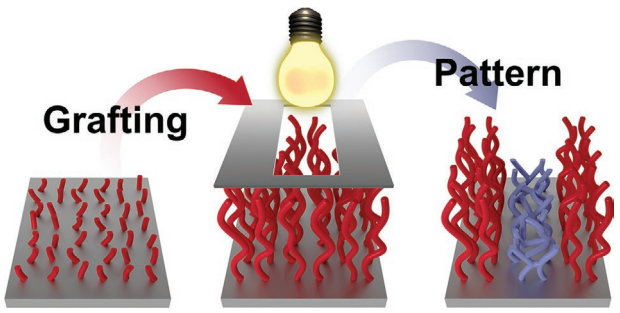

Scheme 1. Light-gated control of conformational changes in polymer brushes grafted from surfaces, from free standing chains (red) to a crosslinked layer (blue).

2. Control of Conformational Changes in *o*-MBA Containing Polymer Brushes

Homogenous polymer brushes bearing statistically distributed *o*-MBA photoreactive moieties in the lateral architecture (**MB**) were synthesized via a literature known surface initiated reversible-deactivation polymerization (SI-RDRP) procedure. Utilising the "grafting-from" approach, polymer brushes were grown from silica surfaces functionalized with a reversible addition fragmentation chain-transfer (RAFT) agent.[33] Comprehensive experimental details on the brush formation can be found in Section S2 of the Supporting Information. The polymer brush consists of poly(methyl methacrylate) (PMMA), which has the photoreactive moiety *o*-MBA statistically incorporated through the polymer with an *o*-MBA containing monomer **M1** (17 mol% incorporation, see Figure S7, Supporting Information). Upon photoexcitation with UV light, the *o*-MBA unit isomerizes to form the reactive species *o*-quinodimethane, which can undergo self-dimerization into various products (**Figure 1**).[34]

To follow the dimerization of the incorporated *o*-MBA moieties upon irradiation with UV light, UV/vis spectra of a surface functionalized quartz cuvette (refer to Section S2.3.5, Supporting Information) containing the *o*-MBA polymer brush were recorded. The polymer brush was swollen in toluene and UV/vis spectra were recorded intermittently during UV irradiation with λ = 325 nm. The reduction of the *o*-MBA absorbance band can be seen in **Figure 2**A. After an irradiation time of 60 min the absorbance maximum at λ = 315 nm, attributed to the *o*-MBA moiety, had disappeared, suggesting that the *o*-MBA dimerization had proceeded close to completion and negligible free *o*-MBA moieties remained in the polymer brush. The performed UV/vis measurements of the polymer brush crosslinking gives valuable chemical confirmation of the dimerization reaction through the depletion of *o*-MBA moieties. However, no direct information of the conformational changes within the brush can be deduced from UV/vis measurements.

Further investigations of polymer brushes on planar silicon surfaces (refer to Section S2.3.4, Supporting Information) via AFM-based colloidal probe measurements demonstrated the change in physical properties of the polymer brush upon UV irradiation (Figure 2B). Through retraction of an AFM cantilever from the surface, the adhesion force between a colloidal probe (3.5 µm SiO_2 particle) and the polymer brush can be determined. For the full experimental details refer to

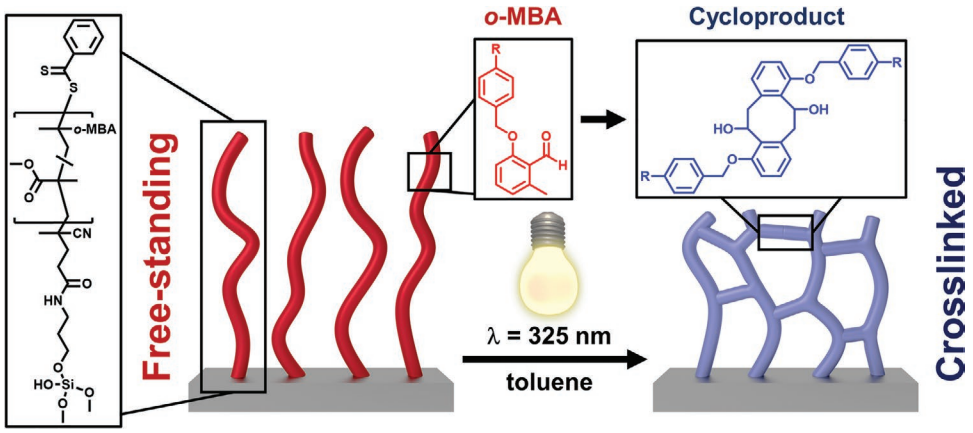

Figure 1. Schematic representation of the conformational change of **MB** polymer brushes through photochemical intermolecular crosslinking of grafted polymer chains containing *o*-MBA moieties.

Section S1.7 of the Supporting Information. A distinct change in adhesion force, from −500 pN for the non-irradiated polymer brush to almost 0 pN for the UV-light irradiated sample, was observed. The substantial difference in adhesion force can be explained by the loss of freestanding polymer ends in the crosslinked polymer brush.[32] Freestanding polymer ends can readily adhere to a colloidal probe and result in higher adhesion between the polymer brush and the AFM probe. The AFM-based colloidal probe measurements provide the first indication of light-gated conformational changes in the polymer brushes.

In-depth investigation of the light-gated conformational change of polymer brushes can be achieved with the aid of neutron reflectometry (NR). NR measurements were performed on the previously described **MB** structures and **DB** structures containing PMMA with and without the photoreactive moiety *o*-MBA, respectively. The evaluation of the NR spectra was performed with refnx[35,36] and a comprehensive summary of underlaying calculations can be found in Section S1.4 of the Supporting Information. The change in the modeled volume fraction profiles of the **MB** and **DB** polymer brushes before and after irradiation at λ = 325 nm can be explained by a change of conformation through crosslinking, and the accompanying redistribution of density relative to distance from the surface throughout the entire *o*-MBA containing block (**Figure 3**, thickness and volume fraction). An increase in density (compression of the polymer volume fraction) combined with a decrease in swollen thickness from 65 to 50 nm can be seen in Figure 3A, explained by the light triggered crosslinking of the **MB** structure (schematic representation at the bottom). For the two more complex **DB** structures a distinct difference of the volume fraction profile after irradiation can be observed in Figure 3B,C (blue curves). The **DB1** structure, with the "active block" (*o*-MBA copolymerized with MMA) at the bottom and the "passive block" (only MMA) at the top, shows a strong increase in density close to the substrate surface (Figure 3B) whereas the inverse **DB2** structure show a noticeable higher density further away from the surface (Figure 3C). Schematic representations of the crosslinking of the **DB** structures are depicted at the bottom (Figure 3B,C). The performed UV/vis, AFM, and NR crosslinking experiments collectively confirm light triggered changes in polymer brush conformation via chemical crosslinking reactions. Additionally, the tested **DB** structures show an additional level of control in the *z*-direction within predefined areas of crosslinking through sequential "grafting from" SI-RDRP.

Having demonstrated the ability to induce confirmational changes in polymer brushes postmanufacturing, we now turn to accessing 2D spatiotemporal control. To demonstrate this spatiotemporal control over crosslinking, a predetermined area of an **MB** polymer brush on a silicon substrate was irradiated with UV light using a photomask. Detailed experimental procedures are summarized in Section S3.1 of the Supporting Information. Time of flight (ToF) secondary ion mass spectrometry (SIMS) measurements were employed to assess the spatial resolution of the chemical crosslinking. ToF-SIMS images of the irradiated samples reveal significant differences in the chemical composition of the irradiated and non-irradiated areas. In **Figure 4**A, the non-irradiated areas show a high abundance of fragments assigned to the *o*-MBA photoreactive moiety, which are not present in the irradiated area due to light induced dimerization. Figure 4B shows the presence of the dimer fragments exclusively in the irradiated areas of the sample. The overlay of the sum of significant fragments for the *o*-MBA moieties (red area—Figure 4C) and dimerized species (blue area—Figure 4C) confirms the spatiotemporal control over the chemical composition of the crosslinks and hence the light-gated conformational change in the polymer brushes.

3. In Situ Change of Conformation in MB and DB Brushes via QCM-D

To gain further insight into the kinetics of the conformational changes in the polymer brushes, additional in situ measurements were performed employing a hyphenated nanoplasmonic sensing (NPS)[37,38] QCM-D.[39,40] In addition to online monitoring, QCM-D measurements provide further understanding of the underlying changes in the physical properties of the polymer brush, i.e., stiffness, density, and optical mass. A detailed description of the complete experimental setup and the grafting of polymer brushes from QCM sensors can be found in Section S1.3 of the Supporting Information.

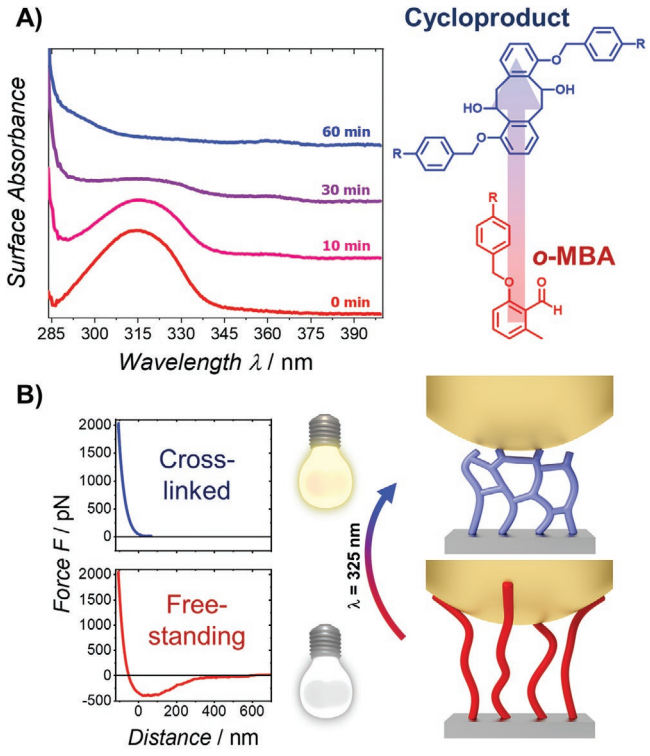

Figure 2. A) UV/vis spectra of a crosslinked monoblock polymer brush (**MB**) via dimerization of *o*-MBA photoreactive moieties (reduction of *o*-MBA absorbance band with increasing irradiation time) at a wavelength of $\lambda = 325$ nm on a quartz cuvette. B) AFM-based colloidal probe measurements on freestanding and crosslinked polymer brushes, adhesion force recorded through cantilever retraction (schematic representations not-to-scale).

The NPS QCM-D setup enables the parallel in situ recording of frequency, dissipation and nanoplasmonic changes of the polymer brush during irradiation (see **Figure 5**). QCM-D measurements of the functionalized sensors containing the **MB** polymer brushes were recorded starting with dry measurements, keeping the sensors in the dark. Once the base line had stabilized, toluene was passed over the sensors until the brushes equilibrated in the flow, at which point irradiation experiments were conducted in a swollen state of the brushes. The optics unit of the NPS system ($\lambda = 300$–880 nm) was found to be sufficient to induce an initial conformational change in the polymer brush (Figure 5A), whilst parallel recording the NPS wavelength. By turning the NPS light source on and off, temporal control over the conformational change in the polymer brush could be demonstrated. Subsequent irradiation with a UV LED (λ = 325 nm, Figure 5B) triggered the crosslinking of any unreacted *o*-MBA and completed the conformational change of the polymer brush. The negligible change in the wavelength of the NPS measurement (Figure 5A bottom graph) indicates that the optical mass of the polymer brush is not changing significantly during irradiation.[41] The increase in resonance frequency and decrease in dissipation, recorded via QCM-D, without any change in mass (dimerization of *o*-MBA moieties result in no mass change),[34] suggests an increase in density and stiffness of the polymer brush above the QCM sensor. These results confirm a thinner, denser layer is formed, which can only be explained through the presence of intermolecular crosslinks. The difference of the crosslinking kinetics between the NPS optics and the UV LED-induced conformational change can be explained by the comparatively low photon flux in the UV range of the NPS halogen lamp (refer to the emission spectrum, Section S1.3, Supporting Information) relative to the employed UV LED.

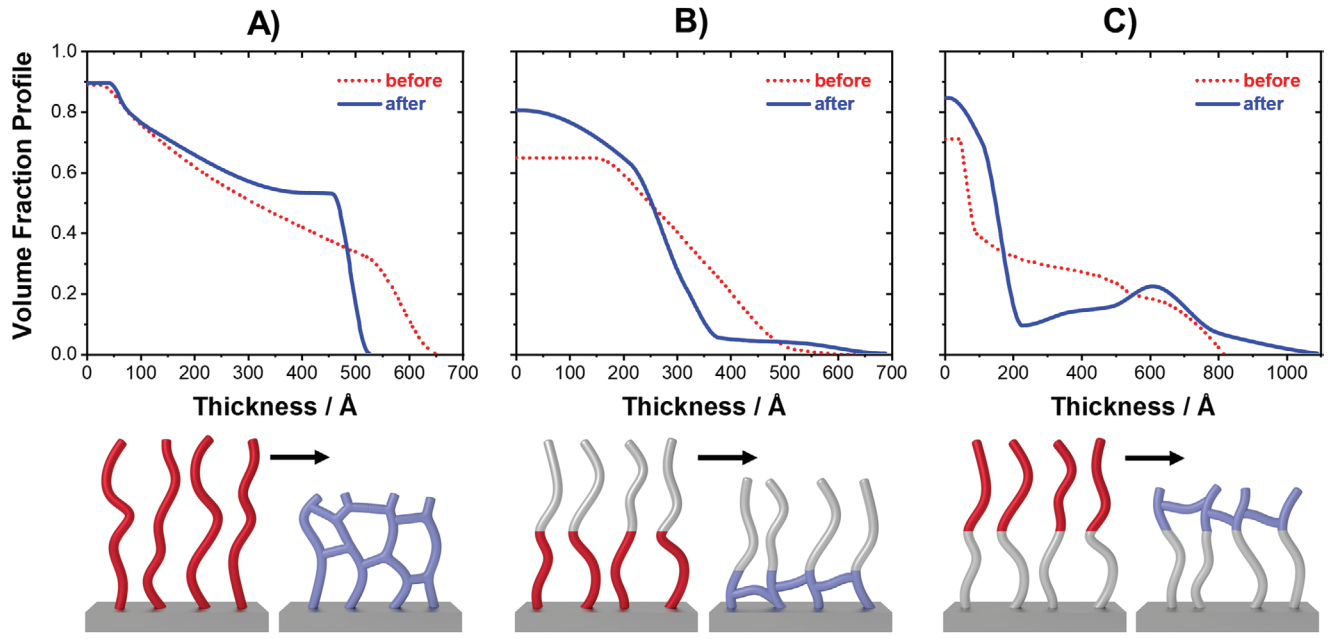

Figure 3. Volume fraction profiles determined via NR measurements before (red dotted lines) and after (blue solid lines) photochemical crosslinking of *o*-MBA containing free standing chains (red to blue block). A) **MB** structure, B) **DB1** structure with *o*-MBA containing block at the bottom and PMMA passive block (white blocks) at the top, and C) **DB2** structure with PMMA passive block at the bottom and *o*-MBA containing block at the top.

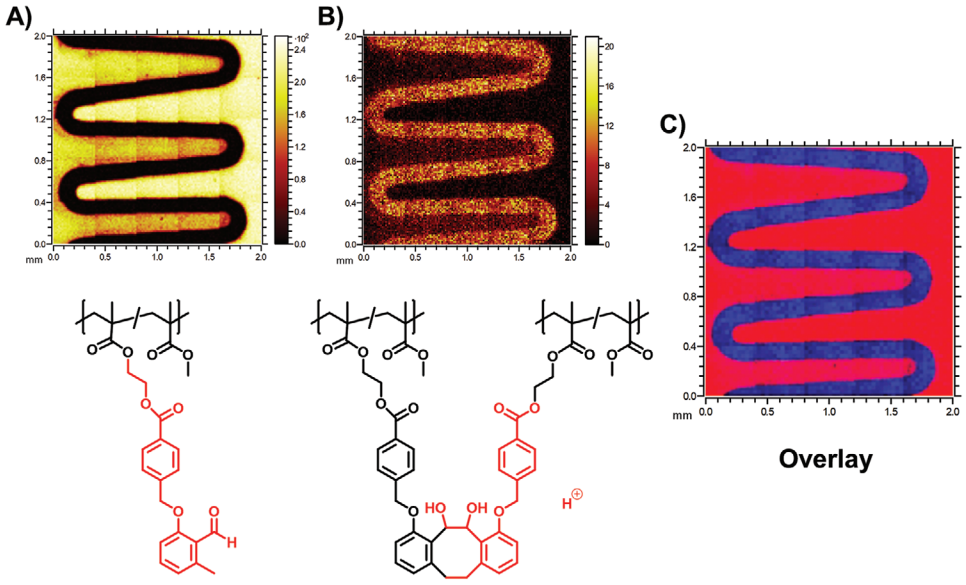

Figure 4. ToF-SIMS images of A) the *o*-MBA moiety (positive mode) and B) the dimerized/crosslinked *o*-MBA (positive mode), along with the respective chemical structures of the monitored ionized fragments (in red). C) Overlayed image with blue all possible *o*-MBA dimer fragments ($C_{19}H_{19}O_4^+$, $C_{19}H_{21}O_5^+$) and red all *o*-MBA fragments ($C_{18}H_{17}O_4^+$, $C_{18}H_{18}O_4^+$, $C_{16}H_{13}O_3^+$, $C_9H_9O_2^+$).

To further extend the conformational control over the block copolymer brushes, a second photoreactive moiety (StyP) was incorporated into the polymer brushes. The λ-orthogonal addressability of the StyP and *o*-MBA moieties has been investigated in our previous studies, where we demonstrated that both photoreactions can be induced exclusively by employing different excitation wavelengths.[42,43] Upon visible light irradiation, StyP forms a [2 + 2] cycloproduct, whereas the dimerization was reported to be suppressed in the UV region where the *o*-MBA moiety is triggered. Incorporating each group into a specific block of a dual block copolymer brush structure offers the potential for an additional level of conformational control

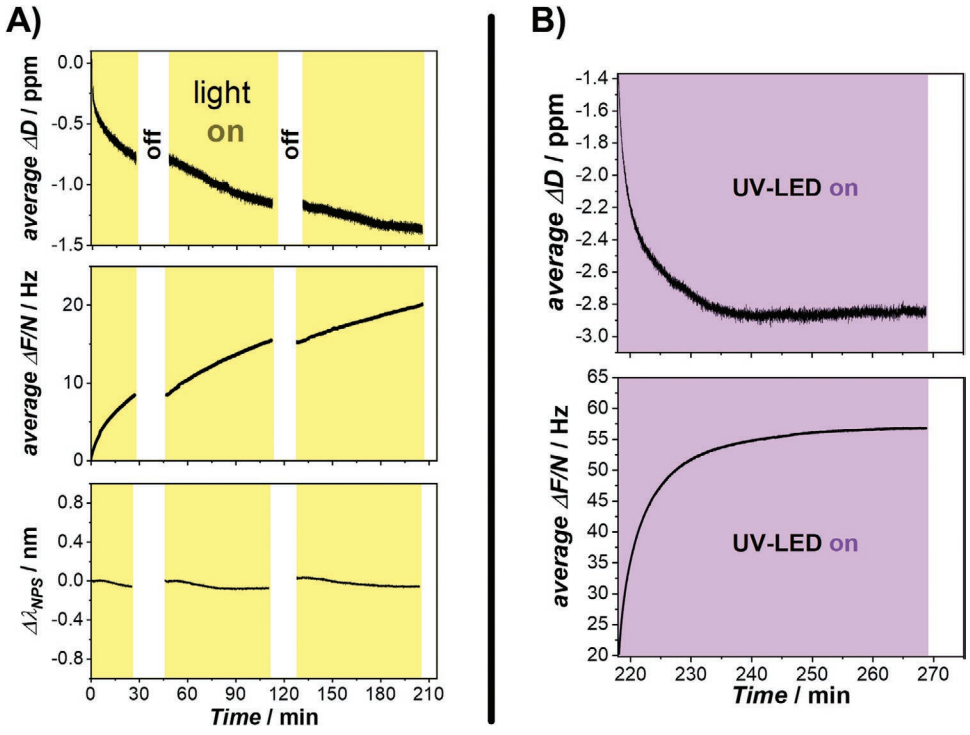

Figure 5. In situ QCM-D and NPS measurements on the crosslinking of *o*-MBA containing polymer brushes with an increase in frequency, decrease in dissipation and constant NPS wavelength. A) For the first three time periods the NPS light (λ = 300–880 nm) was employed to induce crosslinking followed by B) UV-LED (λ = 325 nm) irradiation for fast completion of crosslinking reaction.

over the previously presented **DB** polymer brushes. Here, we expand on the "active" and "passive" block architecture by incorporating two individually accessible photoactive blocks. Then, with the careful selection of applied wavelength, not only can the individual blocks be crosslinked, but rather both blocks in a sequence dependent fashion. To investigate the conformational control of the diblock copolymer brushes, additional QCM-D experiments were conducted.

The diblock copolymer brushes **DB*** were prepared on functionalized QCM sensors consisting of a first b lock o f MMA statistically copolymerized with StyP containing monomer **M2** (**Figure 6**, black polymer chains) and a second block of MMA statistically copolymerized with the *o*-MBA containing monomer **M1** (Figure 6, red polymer chains) using the SI-RAFT approach. Subsequently, QCM-D measurements were performed as described above. The change in dissipation was measured in situ while sequentially irradiating the blocks, by either irradiating first w ith v isible l ight f ollowed by UV irradiation (Figure 6, right dissipation graph) or vice versa (Figure 6, left dissipation graph). For more details refer to Section S1.3 of the Supporting Information. By inducing the visible light-gated dimerization of StyP moieties first (crosslinking of lower block in copolymer brush), an initial decrease in dissipation energy was recorded, similar to the UV light induced crosslinking of the *o*-MBA monoblock polymer brushes **MB** (Figure 5B). An additional, subsequent conformational change of the upper polymer block was achieved by UV irradiation (refer to the two distinct steps in the dissipation change in Figure 6, right dissipation graph). These results indicate that it is possible to selectively crosslink specific parts of the polymer brush architecture by choice of irradiation wavelength, through incorporation of wavelength selective photoreactive moieties in the lateral structure of the polymer chain. When the irradiation sequence was inverted and the same brush structure was irradiated with UV light first immediate crosslinking of both photoreactive moieties took place simultaneously. Further irradiation with visible light did not result in a significant change of the brush conformation (see Figure 6, left dissipation graph). The in situ measurements of the photoinduced crosslinking of the brushes not only demonstrates that a change in energy dissipation of the crosslinked polymer brushes give insights into the conformational changes of their structure (crosslinks between the polymer brushes of a block result in reduced dissipation), but also highlights the loss of the sequence-independent irradiation pathway, which was previously reported in highly confined macromolecular environments of single chain nanoparticles.[44] While both crosslinking reactions can only be induced selectively in a sequence of decreasing irradiation wavelength, the control over the crosslinking sequence of upper and lower block can be readily adjusted by synthetically inverting the distribution of photochemical gates in the two polymer blocks.

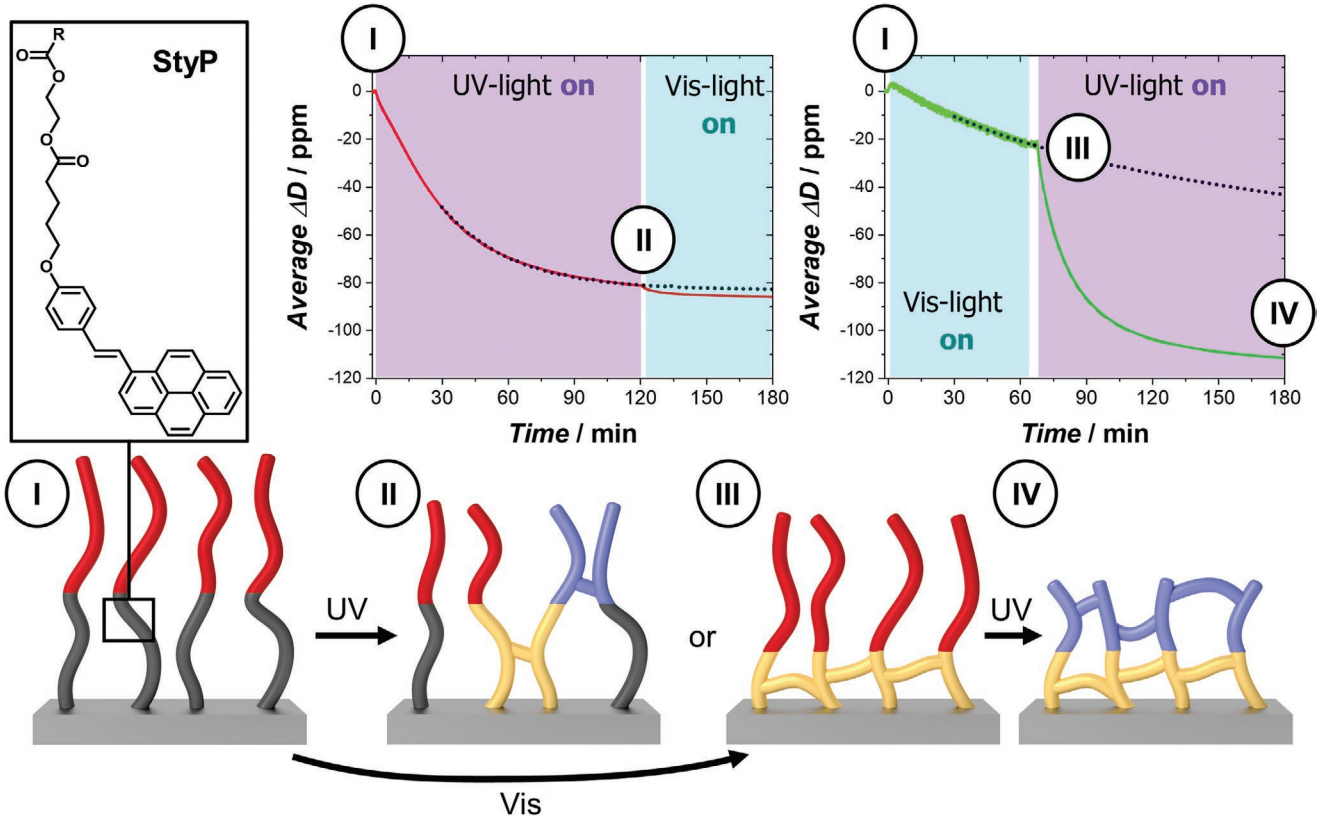

Figure 6. QCM dissipation measurements on diblock copolymer brushes **DB*** containing StyP crosslinking moieties in the lower block and *o*-MBA crosslinking moieties in the upper block with crosslinking induced by first UV light ($\lambda = 325$ nm) followed by vis light ($\lambda = 445$ nm) irradiation or second vis light ($\lambda = 445$ nm) followed by UV light ($\lambda = 325$ nm) irradiation.

4. Conclusions

We demonstrate through comprehensive surface characterization that the incorporation of photoreactive *o*-MBA units into surface tethered polymers enables spatiotemporal control over the crosslinking and conformation of polymer brushes. Precise control over conformational changes in polymer brushes can be achieved through predetermined "active" blocks in the brush structure via SI-RDRP. By incorporating a second photogate into the lower block of the polymer brush, an even higher degree of control over the *z*-dimension is achieved. By initial irradiation with visible light, the lower part of the brush was selectively crosslinked through the photodimerization of StyP, while the upper part was subsequently crosslinked by irradiation with UV light triggering the *o*-MBA reaction. While these two photoreactive moieties displayed irradiation sequence-independent crosslinking in solution and photoresists, the space confinements i n t he p olymer b rushes p revented a s equence independent addressability. As a consequence, initial irradiation with the shorter wavelength induces crosslinking of both blocks at the same time.

The introduced technology allows the utilization of surface patterned polymer brushes in a wide variety of application fields. The light-induced changes of conformation are accompanied with distinct differences in surface properties and can be tailored by adjusting the SI-RDRP process. We submit that by incorporating photocrosslinking moieties, which preserve their sequence-independent addressability within the confined environment of polymer brushes, control of conformational changes in three dimensions becomes possible.

Supporting Information

Supporting Information is available from the Wiley Online Library or from the author.

Acknowledgements

C.B.-K. is grateful for an Australian Research Council (ARC) Laureate Fellowship enabling his photochemical research program as well as continued key support from the QUT. C.B.-K. acknowledges funding in the context of an ARC Discovery project. H.F. gratefully acknowledges generous funding from the ARC in form of a DECRA Fellowship. T.K. gratefully acknowledges funding by the Leopoldina Fellowship Programme, German National Academy of Sciences Leopoldina (LPDS-2017-05). The Central Analytical Research Facility (CARF) at QUT is gratefully acknowledged for access to analytical instrumentation. The authors are grateful for the beamtime grant and strong support from Australian Nuclear Science and Technology Organisation (ANSTO). L.M. gratefully acknowledges Insplorion and ATA Scientific for access to the NPS device.

Conflict of Interest

The authors declare no conflict of interest.

Data Availability Statement

Research data are not shared.

Keywords

crosslinking, photochemistry, polymer brush, surface characterization, surface patterning

[1] R. R. Matheson, Jr. *Science* **2002**, *297*, 976.
[2] K. Yu, J. C. Y. Lo, Y. Mei, E. F. Haney, E. Siren, M. T. Kalathottukaren, R. E. W. Hancock, D. Lange, J. N. Kizhakkedathu, *ACS Appl. Mater. Interfaces* **2015**, *7*, 28591.
[3] J. E. Raynor, J. R. Capadona, D. M. Collard, T. A. Petrie, A. J. García, *Biointerphases* **2009**, *4*, FA3.
[4] M. O'Neill, S. M. Kelly, *J. Phys. D: Appl. Phys.* **2000**, *33*, R67.
[5] M. Kobayashi, A. Takahara, *Chem. Rec.* **2010**, *10*, 208.
[6] R. M. Bielecki, M. Crobu, N. D. Spencer, *Tribol. Lett.* **2013**, *49*, 263.
[7] W. J. Yang, K.-G. Neoh, E.-T. Kang, S. L.-M. Teo, D. Rittschof, *Prog. Polym. Sci.* **2014**, *39*, 1017.
[8] K. Matyjaszewski, *Prog. Polym. Sci.* **2005**, *30*, 858.
[9] M. Motornov, S. Minko, K. J. Eichhorn, M. Nitschke, F. Simon, M. Stamm, *Langmuir* **2003**, *19*, 8077.
[10] T. Drobek, N. D. Spencer, *Langmuir* **2008**, *24*, 1484.
[11] L. Michalek, L. Barner, C. Barner-Kowollik, *Adv. Mater.* **2018**, *30*, 1706321.
[12] L. Michalek, K. Mundsinger, C. Barner-Kowollik, L. Barner, *Polym. Chem.* **2019**, *10*, 54.
[13] C. J. Hawker, Z. A. Page, P. Trefonas, A. N. Sokolov, J. Kramer, D. S. Laitar, S. Mukhopadhyay, B. Narupai, C. W. Pester, *US 10,211,400 B2*, **2019**.
[14] H. Robertson, E. C. Johnson, I. J. Gresham, S. W. Prescott, A. Nelson, E. J. Wanless, G. B. Webber, *J. Colloid Interface Sci.* **2021**, *586*, 292.
[15] S. Sanjuan, P. Perrin, N. Pantoustier, Y. Tran, *Langmuir* **2007**, *23*, 5769.
[16] E. S. Dehghani, S. Aghion, W. Anwand, G. Consolati, R. Ferragut, G. Panzarasa, *Eur. Polym. J.* **2018**, *99*, 415.
[17] P. Mocny, H.-A. Klok, *Macromolecules* **2020**, *53*, 731.
[18] G. Dunér, E. Thormann, O. Ramström, A. Dėdinaitė, *J. Dispersion Sci. Technol.* **2010**, *31*, 1285.
[19] D. M. Loveless, N. I. Abu-Lail, M. Kaholek, S. Zauscher, S. L. Craig, *Angew. Chem., Int. Ed.* **2006**, *45*, 7812.
[20] S. Micciulla, J. Michalowsky, M. A. Schroer, C. Holm, R. von Klitzing, J. Smiatek, *Phys. Chem. Chem. Phys.* **2016**, *18*, 5324.
[21] S. N. Ramakrishna, M. Cirelli, E. S. Kooij, M. Klein Gunnewiek, E. M. Benetti, *Macromolecules* **2015**, *48*, 7106.
[22] E. S. Dehghani, N. D. Spencer, S. N. Ramakrishna, E. M. Benetti, *Langmuir* **2016**, *32*, 10317.
[23] I. Lilge, H. Schönherr, *Eur. Polym. J.* **2013**, *49*, 1943.
[24] H. Frisch, D. E. Marschner, A. S. Goldmann, C. Barner-Kowollik, *Angew. Chem., Int. Ed.* **2018**, *57*, 2036.
[25] M. Fromel, M. Li, C. W. Pester, *Macromol. Rapid Commun.* **2020**, *41*, 2000177.
[26] B. Narupai, Z. A. Page, N. J. Treat, A. J. McGrath, C. W. Pester, E. H. Discekici, N. D. Dolinski, G. F. Meyers, J. Read de Alaniz, C. J. Hawker, *Angew. Chem., Int. Ed.* **2018**, *57*, 13433.
[27] E. H. Discekici, C. W. Pester, N. J. Treat, J. Lawrence, K. M. Mattson, B. Narupai, E. P. Toumayan, Y. Luo, A. J. McGrath, P. G. Clark, J. Read De Alaniz, C. J. Hawker, *ACS Macro Lett.* **2016**, *5*, 258.
[28] Y. S. Zholdassov, D. J. Valles, S. Uddin, J. Korpanty, N. C. Gianneschi, A. B. Braunschweig, *Adv. Mater.* **2021**, *33*, 2100803.

[29] C. Carbonell, D. Valles, A. M. Wong, A. S. Carlini, M. A. Touve, J. Korpanty, N. C. Gianneschi, A. B. Braunschweig, *Nat. Commun.* **2020**, *11*, 1244.
[30] M. Li, M. Fromel, D. Ranaweera, S. Rocha, C. Boyer, C. W. Pester, *ACS Macro Lett.* **2019**, *8*, 374.
[31] G. Ng, P. Judzewitsch, M. Li, C. W. Pester, K. Jung, C. Boyer, *Macromol. Rapid Commun.* **2021**, 2100106.
[32] L. Michalek, T. Krappitz, K. Mundsinger, S. L. Walden, L. Barner, C. Barner-Kowollik, *J. Am. Chem. Soc.* **2020**, *142*, 21651.
[33] T. Tischer, R. Gralla-Koser, V. Trouillet, L. Barner, C. Barner-Kowollik, C. Lee-Thedieck, *ACS Macro Lett.* **2016**, *5*, 498.
[34] T. Krappitz, F. Feist, I. Lamparth, N. Moszner, H. John, J. P. Blinco, T. R. Dargaville, C. Barner-Kowollik, *Mater. Horiz.* **2019**, *6*, 81.
[35] I. J. Gresham, T. J. Murdoch, E. C. Johnson, H. Robertson, G. B. Webber, E. J. Wanless, S. W. Prescott, A. R. J. Nelson, *J. Appl. Crystallogr.* **2021**, *54*, 739.
[36] A. R. J. Nelson, S. W. Prescott, *J. Appl. Crystallogr.* **2019**, *52*, 193.
[37] G. J. Ma, A. R. Ferhan, J. A. Jackman, N.-J. Cho, *Langmuir* **2020**, *36*, 10606.
[38] G. M. L. Messina, B. Di Napoli, M. De Zotti, C. Mazzuca, F. Formaggio, A. Palleschi, G. Marletta, *Langmuir* **2019**, *35*, 4813.
[39] R. Ortiz, S. Olsen, E. Thormann, *Langmuir* **2018**, *34*, 4455.
[40] G. Zhang, C. Wu, *Macromol. Rapid Commun.* **2009**, *30*, 328.
[41] J. A. Jackman, A. Rahim Ferhan, N. Cho, *Chem. Soc. Rev.* **2017**, *46*, 3615.
[42] S. Bialas, L. Michalek, D. E. Marschner, T. Krappitz, M. Wegener, J. Blinco, E. Blasco, H. Frisch, C. Barner-Kowollik, *Adv. Mater.* **2019**, *31*, 1807288.
[43] L. Michalek, S. Bialas, S. L. Walden, F. R. Bloesser, H. Frisch, C. Barner-Kowollik, *Adv. Funct. Mater.* **2020**, *30*, 2005328.
[44] H. Frisch, J. P. Menzel, F. R. Bloesser, D. E. Marschner, K. Mundsinger, C. Barner-Kowollik, *J. Am. Chem. Soc.* **2018**, *140*, 9551.